

# Experimental Studies of Leak Pressure of FRP Butt Joint between Two Aluminum Pipes

R. N. Ladhwe<sup>1</sup> Shantanu Ladhwe<sup>2</sup> Narendra Kulkarni<sup>3</sup> Dr. Raju Narayanrao Ladhwe<sup>4</sup>  
<sup>4</sup>Associate Professor

<sup>1,2,3,4</sup>Department of Mechanical Science

<sup>1,4</sup>College of Engineering, Shivajinagar, Pune, Maharashtra, 411005, India <sup>2,3</sup>Modern Education Society's College of Engineering, Pune, Maharashtra, 411001, India

**Abstract**—A FRP butt-joint was formed between two adherends of aluminium pipe of outside diameter of 25.40 mm and inside diameter of 22.20 mm. The joint was formed by winding a wetted roving of glass fiber / carbon fiber with controlled quantity of epoxy at  $\pm 45^\circ$  angle. It was cured to form the joint with a glass fiber reinforced polymer (GFRP) / carbon fiber reinforced polymer (CFRP) sleeve around the joint plane. For checking leakages in this joint dead weight pressure gauge tester was used. It can be inferred that pressure at which leakage takes place through FRP joint is directly proportional to the number of passes of glass / carbon fiber roving. It is because when number of passes of glass fiber increases, more compact FRP joint is formed which can undertake more pressure. Specimen with lesser number of passes of glass fiber / carbon fiber, leak through center of FRP joint while specimen of higher number of passes leak through either upper or lower side of FRP joint. During leak test, when the pressure inside the aluminium pipe increases, hoop stress also increase leading to expansion of aluminium pipe thereby forming the strong matrix of FRP. This formation of strong matrix increases the pressure at which leak occurs i.e. it enhances the results.

**Key words:** FRP Joint, Adherends, GFRP, CFRP, Leak Test

## I. INTRODUCTION

The world needs pipe to survive for water, oil, gas and sewage. Pipes have been a fundamental part of civilization since 3,000 BC as the world have developed, both in terms of population and infrastructure. Today, we are reliant on water, gas, oil and electricity and pipes carry these materials from their source to their users. Whenever two pipes need to be joined together, butt joint is the answer. Butt joint is typically used in process piping & heavier industrial applications. The joints between pipes are likely to leak. Presence of the leakage will bring out the further problems such as safety of the system, also problem regarding the function and reliability of the system in particular. If a leak is found in piping system, it is possible to slow down or temporarily stop the leakage until the plumber can repair by the ordinary methods. Thus, there is a need to find an economical, fast rugged and reliable solution for the same. The butt joint by FRP has a potential to meet these requirements.

Kumar et al. [1] & [2] developed FRP-joints made between two components by winding a wetted tow made of high strength and high stiffness glass fibers. A T-joint between two pipes was selected as a specimen. The strength of the T-joint was determined under four loading conditions: (i) tensile, (ii) in-plane bending, (iii) bending under a transverse load, and (iv) torsion-cum-bending. The strength of FRP-joint between mild steel pipes was found to be comparable to the strength of a welded joint. Ramkumar et al. [3] developed a GFRP butt joint between two pipes by

wrapping a wetted glass fabric and letting it to get cured. They found the joint to be strong against flexural loads but weak under tensile loads.

Imanaka et al. [4] investigated the behaviour of adhesively bonded GFRP pipe/steel rod joints and found that fatigue strength of the joint mainly depended on maximum tensile stress normal to the adhesive adherend interface at the lap end. Jiao et al. [5] studied the behaviour of butt-welded joint between very high strength (VHS) circular steel tubes, strengthened by GFRP and found that the joint failed with three kinds of modes, adhesive failure, fiber tear and mixed failure. Fawzia et al. [6] also studied the behaviour of very high strength (VHS) circular steel tubes strengthen by carbon fiber reinforced polymer (CFRP) under axial tension and effective bond length of CFRP reinforcement was established. Zhaoa and Zhang [7] reviewed articles on fatigue crack propagation in the GFRP-steel system. Raykhere et al. [8] evaluated the dynamic shear strength of adhesive joints prepared using four different commercial adhesives at loading rates in the range of 0.6–1.2 MPa/ $\mu$ s. Ladhwe et al. [9] formed GFRP butt joint between similar materials, aluminum and was characterized under tensile and flexural loading. Ladhwe et al. [10] developed butt joint between the pipes of dissimilar materials, aluminum and steel using carbon fiber roving. The joint was tested experimentally under tensile and flexural loading. The experimental results were interpreted on the basis of numerical analysis carried out using ANSYS. W. Hufenbach, R. Böhm [11], has analysed that due to their high lightweight potential, fiber reinforced plastics have found a broad application in chemical apparatus and plant construction. Because of improved standards for safety, reliability and cost effectiveness of such composite components, numerous technical challenges arise for the producers of pressure vessels, tanks, reactors and pipe element systems. In this context, a multitude of problems appear during recurring acceptance inspections and equipment condition monitoring using non-destructive test methods (leak detection method).

The objective of the work is to develop a butt joint between two aluminium pipes by winding glass fiber / carbon fibers roving, wetted in epoxy resin, and letting it cured to form a glass fiber reinforced polymer (GFRP) / carbon fiber reinforced polymer (CFRP) sleeve. The butt joint was tested for leak pressure using Dead Weight Pressure Gauge Testers.

## II. EXPERIMENTAL TECHNIQUE

The specimen used for leakage test was developed butt joint, by joining two aluminum pipes with a glass / carbon roving reinforced epoxy material. For checking leakages in this joint dead weight pressure gauge tester was used. A dead weight tester is a calibration standard method that uses

a piston cylinder on which a load is placed to make equilibrium with an applied pressure underneath the piston.

**A. Materials**

Commercially available aluminum pipes were used as the adherends in this study, whose properties were: elastic modulus = 69 GPa, poisson’s ratio = 0.33, yield stress = 152 MPa, and ultimate tensile strength = 183 MPa. Each adherend member was of 25.40 mm outside diameter, 22.20 mm inside diameter and 175 mm length. The glass fiber roving used was of 1200 Tex and purchased from Owens Corning India Limited, Raigad India. The carbon fiber roving used for preparing specimen was of 210 Tex, manufactured by Hexcel Corporation, 6700 West 5400 South West Valley City, UT 84118, USA. The epoxy resin employed was Dobeckot 520 F (100 parts by weight) with hardener Beck 758 (9 parts by weight). The mixture of epoxy resin and hardener enabled convenient processing time of 25-30 minutes.

**B. FRP winding**

To prepare the specimen by winding wetted glass / carbon roving, a FRP-winding setup was developed. The mating faces of the aluminum and the steel pipes were machined normal to their axes and were placed in a specially designed winding setup. It was used to carry out the following two major functions, (i) to wet the fiber roving with controlled amount of epoxy resin and (ii) to wind the wetted roving. The external surfaces of both the pipes were made rough using a file in  $\theta$ -direction (normal to axis of pipes). Then the surfaces were cleaned with acetone so as to degrease them. To control the fiber volume fraction, the wetted roving was passed through a specially designed die with a hole having an enlarged conical mouth for the smooth entry of the roving.

Three kinds of winding angles were employed,  $\pm 45^\circ$ ,  $\pm 70^\circ$  and  $90^\circ$  C loops shown in Figure 1. Windings of  $\pm 45^\circ$  and  $\pm 70^\circ$  were running winding from one adherend to another. It was important to develop strong adhesion between the adherends and the FRP sleeve. After many alternative trials, it was found that good adhesion was developed when the end points of running winding was pressed by two local loops of  $90^\circ$  winding. Passes of  $\pm 45^\circ$  winding, played a major role in the FRP joint, but it was found that four passes initially of  $\pm 70^\circ$  winding were helpful in enhancing the adhesion. Thus, the four passes of  $70^\circ$  winding constituted the preparatic windings over which main winding of  $\pm 45^\circ$  was carried out. The configuration of the preparatic winding was  $[902/ (70/902/ -70/902)2]$  and the configuration of the main winding was  $[45/ 902/-45/902]$  in which n was a large number and was varied in the characterization of the FRP joint. Then the specimen was allowed to be cured for 24 hours at the room temperature. The winding process formed a FRP sleeve of about 130 mm length. The specimen was placed in an oven for the post curing process for 5 hours at the temperature of  $80^\circ$  C. Two kinds of specimen were prepared in this study: (i) Al-GFRP-Al and (ii) Al-CFRP-Al in this investigation. Figure 2 and Figure 3 shows the photographs of the prepared specimens of both kinds.

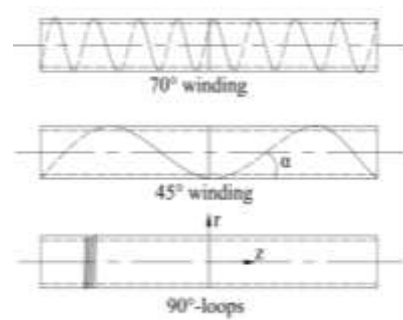


Fig. 1: Various winding loops: 70°, 45° and C-loop



Fig. 2: Photograph of the specimen Al-GFRP-Al



Fig 3: Photograph of the specimen Al-CFRP-Al

A GFRP sleeve is an orthotropic material whose stress-strain relations are expressed with nine elastic constants. They were evaluated using the rule of mixture and Halpin-Tsai equations [12]. The elastic constants, thus determined with respect to principal material axes L, T and T' directions, are listed in Table 1.

$E_L$ , GPa	$E_T$ , GPa	$E_{T'}$ , GPa	$\nu_{LT}$	$\nu_{LT'}$	$\nu_{TT'}$	$G_{LT}$ , GP a	$G_{LT'}$ , GP a	$G_{TT'}$ , GP a
39.47	12.97	12.97	0.276	0.276	0.4	3.89	3.89	4.63

Table 1: Elastic constants of GFRP sleeve material with respect to material axes L, T and T'.

The elastic constants of CFRP were determined with respect to principal material axes L, T and T' directions, and are listed in Table 2.

$E_L$ , GPa	$E_T$ , GPa	$E_{T'}$ , GPa	$\nu_{LT}$	$\nu_{LT'}$	$\nu_{TT'}$	$G_{LT}$ , GP a	$G_{LT'}$ , GP a	$G_{TT'}$ , GP a
99.22	11.39	11.39	0.292	0.292	0.4	3.30	3.30	4.06

Table 2: Elastic properties of CFRP with respect to principal material directions L, T and T'.

The stiffness matrix was then evaluated using the elastic constants with respect to principal material axes [13, 14]. The stiffness matrix was then transformed to determine it with respect to global axes r,  $\theta$  and z of a specimen. For the GFRP sleeve, transformed stress-strain relations with respect to global axes r,  $\theta$ , and z were determined as follow: For ply angle  $\beta = 45^\circ$

$$\begin{bmatrix} \sigma_{rr} \\ \sigma_{\theta\theta} \\ \sigma_{zz} \\ \tau_{\theta z} \\ \tau_{rz} \\ \tau_{r\theta} \end{bmatrix} = \begin{bmatrix} 16.43 & 6.84 & 14.24 & 0 & 0 & 6.66 \\ 6.84 & 22.04 & 6.84 & 0 & 0 & 6.66 \\ 14.24 & 6.84 & 22.04 & 0 & 0 & -0.31 \\ 0 & 0 & 0 & 4.26 & -0.36 & 0 \\ 0 & 0 & 0 & -0.36 & 4.26 & 0 \\ 6.66 & 6.66 & -0.31 & 0 & 0 & 11.61 \end{bmatrix} \begin{bmatrix} \epsilon_{rr} \\ \epsilon_{\theta\theta} \\ \epsilon_{zz} \\ \gamma_{\theta z} \\ \gamma_{rz} \\ \gamma_{r\theta} \end{bmatrix}$$

The stiffness constants in Equation are in GPa.

For ply angle  $\beta = -45^\circ$

$$\begin{bmatrix} \sigma_{rr} \\ \sigma_{\theta\theta} \\ \sigma_{zz} \\ \tau_{\theta z} \\ \tau_{rz} \\ \tau_{r\theta} \end{bmatrix} = \begin{bmatrix} 16.43 & 6.84 & 14.24 & 0 & 0 & -6.66 \\ 6.84 & 22.04 & 6.84 & 0 & 0 & -6.66 \\ 14.24 & 6.84 & 22.04 & 0 & 0 & 0.31 \\ 0 & 0 & 0 & 4.26 & 0.36 & 0 \\ 0 & 0 & 0 & 0.36 & 4.26 & 0 \\ -6.66 & -6.66 & 0.31 & 0 & 0 & 11.61 \end{bmatrix} \begin{bmatrix} \epsilon_{rr} \\ \epsilon_{\theta\theta} \\ \epsilon_{zz} \\ \gamma_{\theta z} \\ \gamma_{rz} \\ \gamma_{r\theta} \end{bmatrix}$$

For ply angle  $\beta = 70^\circ$

$$\begin{bmatrix} \sigma_{rr} \\ \sigma_{\theta\theta} \\ \sigma_{zz} \\ \tau_{\theta z} \\ \tau_{rz} \\ \tau_{r\theta} \end{bmatrix} = \begin{bmatrix} 16.43 & 7.09 & 9.72 & 0 & 0 & 0.48 \\ 7.09 & 36.77 & 6.60 & 0 & 0 & 8.08 \\ 9.72 & 6.60 & 16.36 & 0 & 0 & -0.20 \\ 0 & 0 & 0 & 3.98 & -0.23 & 0 \\ 0 & 0 & 0 & -0.23 & 4.54 & 0 \\ 0.48 & 8.08 & -0.20 & 0 & 0 & 7.08 \end{bmatrix} \begin{bmatrix} \epsilon_{rr} \\ \epsilon_{\theta\theta} \\ \epsilon_{zz} \\ \gamma_{\theta z} \\ \gamma_{rz} \\ \gamma_{r\theta} \end{bmatrix}$$

For ply angle  $\beta = -70^\circ$

$$\begin{bmatrix} \sigma_{rr} \\ \sigma_{\theta\theta} \\ \sigma_{zz} \\ \tau_{\theta z} \\ \tau_{rz} \\ \tau_{r\theta} \end{bmatrix} = \begin{bmatrix} 16.43 & 7.09 & 9.72 & 0 & 0 & -0.48 \\ 7.09 & 36.77 & 6.60 & 0 & 0 & -8.08 \\ 9.72 & 6.60 & 16.36 & 0 & 0 & 0.20 \\ 0 & 0 & 0 & 3.98 & 0.23 & 0 \\ 0 & 0 & 0 & 0.23 & 4.54 & 0 \\ -0.48 & -8.08 & 0.20 & 0 & 0 & 7.08 \end{bmatrix} \begin{bmatrix} \epsilon_{rr} \\ \epsilon_{\theta\theta} \\ \epsilon_{zz} \\ \gamma_{\theta z} \\ \gamma_{rz} \\ \gamma_{r\theta} \end{bmatrix}$$

Similarly, transformed stress-strain relations with respect to global axes  $r$ ,  $\theta$ , and  $z$  were determined for the CFRP sleeve as:

For ply angle  $\beta = 45^\circ$

$$\begin{bmatrix} \sigma_{rr} \\ \sigma_{\theta\theta} \\ \sigma_{zz} \\ \tau_{\theta z} \\ \tau_{rz} \\ \tau_{r\theta} \end{bmatrix} = \begin{bmatrix} 13.88 & 5.74 & 28.69 & 0 & 0 & 22.17 \\ 5.74 & 35.29 & 5.74 & 0 & 0 & 22.17 \\ 28.69 & 5.74 & 35.29 & 0 & 0 & 0 \\ 0 & 0 & 0 & 3.68 & -0.38 & 0 \\ 0 & 0 & 0 & -0.38 & 3.68 & 0 \\ 22.17 & 22.17 & 0 & 0 & 0 & 26.24 \end{bmatrix} \begin{bmatrix} \epsilon_{rr} \\ \epsilon_{\theta\theta} \\ \epsilon_{zz} \\ \gamma_{\theta z} \\ \gamma_{rz} \\ \gamma_{r\theta} \end{bmatrix}$$

For ply angle  $\beta = -45^\circ$

$$\begin{bmatrix} \sigma_{rr} \\ \sigma_{\theta\theta} \\ \sigma_{zz} \\ \tau_{\theta z} \\ \tau_{rz} \\ \tau_{r\theta} \end{bmatrix} = \begin{bmatrix} 13.88 & 5.74 & 28.69 & 0 & 0 & -22.17 \\ 5.74 & 35.29 & 5.74 & 0 & 0 & -22.17 \\ 28.69 & 5.74 & 35.29 & 0 & 0 & 0 \\ 0 & 0 & 0 & 3.68 & 0.38 & 0 \\ 0 & 0 & 0 & 0.38 & 3.68 & 0 \\ -22.17 & -22.17 & 0 & 0 & 0 & 26.24 \end{bmatrix} \begin{bmatrix} \epsilon_{rr} \\ \epsilon_{\theta\theta} \\ \epsilon_{zz} \\ \gamma_{\theta z} \\ \gamma_{rz} \\ \gamma_{r\theta} \end{bmatrix}$$

For ply angle  $\beta = 70^\circ$

$$\begin{bmatrix} \sigma_{rr} \\ \sigma_{\theta\theta} \\ \sigma_{zz} \\ \tau_{\theta z} \\ \tau_{rz} \\ \tau_{r\theta} \end{bmatrix} = \begin{bmatrix} 13.88 & 5.74 & 15.22 & 0 & 0 & 2.95 \\ 5.74 & 82.72 & 5.74 & 0 & 0 & 25.55 \\ 15.22 & 5.74 & 14.77 & 0 & 0 & 0 \\ 0 & 0 & 0 & 3.38 & -0.24 & 0 \\ 0 & 0 & 0 & -0.24 & 3.97 & 0 \\ 2.95 & 25.55 & 0 & 0 & 0 & 12.77 \end{bmatrix} \begin{bmatrix} \epsilon_{rr} \\ \epsilon_{\theta\theta} \\ \epsilon_{zz} \\ \gamma_{\theta z} \\ \gamma_{rz} \\ \gamma_{r\theta} \end{bmatrix}$$

For ply angle  $\beta = -70^\circ$

$$\begin{bmatrix} \sigma_{rr} \\ \sigma_{\theta\theta} \\ \sigma_{zz} \\ \tau_{\theta z} \\ \tau_{rz} \\ \tau_{r\theta} \end{bmatrix} = \begin{bmatrix} 13.88 & 5.74 & 15.22 & 0 & 0 & -2.95 \\ 5.74 & 82.72 & 5.74 & 0 & 0 & -25.55 \\ 15.22 & 5.74 & 14.77 & 0 & 0 & 0 \\ 0 & 0 & 0 & 3.38 & 0.24 & 0 \\ 0 & 0 & 0 & 0.24 & 3.97 & 0 \\ -2.95 & -25.55 & 0 & 0 & 0 & 12.77 \end{bmatrix} \begin{bmatrix} \epsilon_{rr} \\ \epsilon_{\theta\theta} \\ \epsilon_{zz} \\ \gamma_{\theta z} \\ \gamma_{rz} \\ \gamma_{r\theta} \end{bmatrix}$$

Stiffness ratio is an important parameter to characterize a FRP joint. Stiffness ratio for the aluminum adherend was defined as

$$S_a = \frac{E_f A_f}{E_a A_a}$$

where  $E_a$  and  $A_a$  represent the elastic modulus and the area of cross section of the aluminum pipe respectively. In the above definition,  $E_f$  of the orthotropic GFRP and CFRP was taken equal to  $C_{33}$  and  $A_f$  is the area of cross section of the  $\pm 45^\circ$  winding which was the main load bearing portion of the sleeve. The stiffness ratio for the various specimens is also shown in result table.

### C. Dead Weight Pressure Gauge Testers

Piping is widely used in chemical and other plants. In some applications, the joints should not allow the leakage of the flow of a liquid inside the tubes. For checking leakages at the joint in the specimen, a dead weight pressure gauge tester was used using lubricant oil. A working of tester was based on calibration method that uses a piston cylinder on which a dead load was placed to make equilibrium with an applied pressure underneath the piston. The instrument, used for leak detection, was manufactured by the RAVIKA instruments, Delhi. The maximum pressure that can be measured by tester was 300 bar. Figure 4 shows the experimental set-up of the dead weight pressure gauge tester.

For carrying out the leak test, initially the specimen was mounted on the 'Dead weight pressure gauge tester' machine. The oil was pumped inside the specimen by using the inbuilt priming pump till it was completely filled with oil and air inside the system was removed. The oil used for the test was SAE-40 Grade. The pressure was increased by adding the dead weights till the leakage occurred through the GFRP/CFRP butt-joint or the pressure reached which would not burst the aluminum adherend.

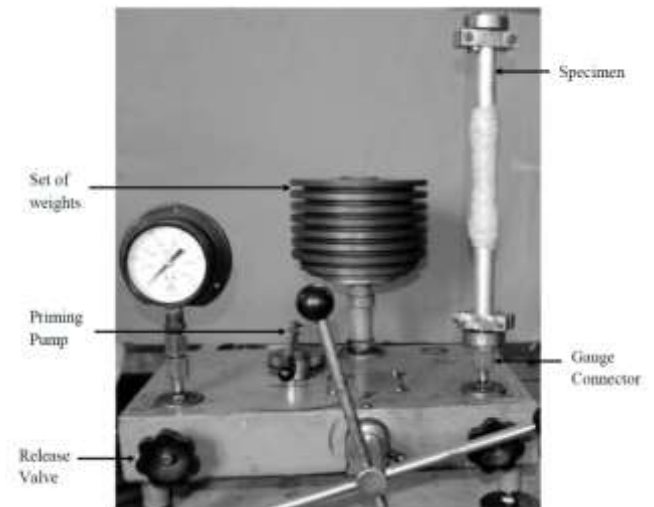


Fig. 4: Experimental Set-up of dead weight pressure gauge tester

#### D. Interfacing Between A Specimen And Testing Machine

A GFRP/CFRP butt-jointed specimen required a proper interfacing so that it could be mounted on the testing machine. A special attachment was designed to conduct the leak test of the butt-joint specimen on the dead weight pressure gauge tester (Figure 5). One end of the specimen was blocked and the other end was required to have a male threaded portion (M 20) so that it could be screwed on the tester. The interface was designed in such way that, it did not leak during the testing. The interface was designed for the maximum pressure of 250 bar. Beyond 250 bar, the aluminum may fail and test may be dangerous.

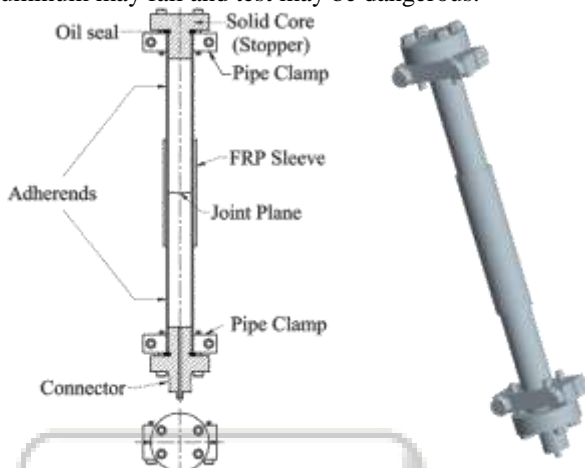


Fig. 5: Sectional view of assembly for leak testing

The assembly is divided into two subassemblies. The upper subassembly blocked the upper end of the specimen while the lower end was suitably designed to be attached to the leak tester. The upper end was blocked by inserting a solid core, shown in Figure 6.

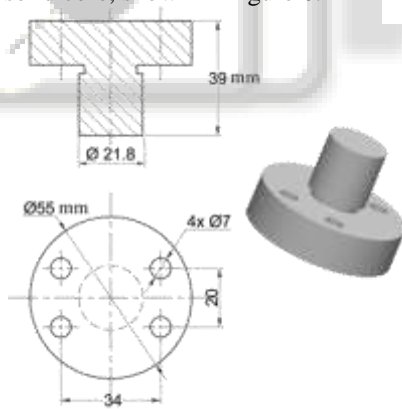


Fig. 6: Sectional view of solid core

The flanged portion of the core was screwed to a pipe clamp attached to the external surface of the pipe using four M6 high strength screws. The pipe clamp was made of two halves (Figure 7) of mild steel. One of them was having tapped holes, M8, and the other one clear holes. To clamp it, the two halves were screwed to the pipe, using high strength alloy steel allen screws. An oil seal made of neoprene was used between the flange and specimen end face to ensure that no oil leaks through. It is flat ring with size 15.87x27.38x3.17 mm. It is worth mentioning here that the core was made long enough in such a way that the pipe clamp did not crush the adherend tube.

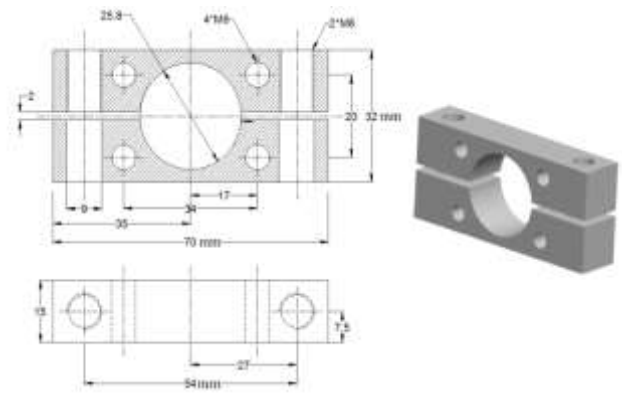


Fig. 7: sectional view of Clamp

In the lower subassembly (Figure 8), the core had a drilled hole of  $\text{Ø} = 2.5 \text{ mm}$  so that the liquid of the tester could enter the specimen. The design of the cored portion and its flange was same as that one used on the blocked end. However, the other end of the core was machined with M20 thread so that it could be screwed to the leak tester. Another pipe clamp was employed to tighten the core to the specimen pipe with an oil seal in between.

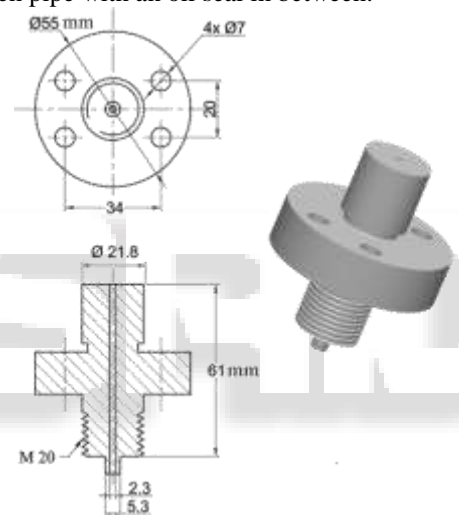


Fig. 8: sectional view of Hollow Core

Figures 9 and 10 shows the photographs of the specimen with both subassemblies for CFRP and GFRP butt joint specimens.



Fig. 9: Photograph of actual assembly GFRP sleeve specimen



Fig. 10: Photograph of actual assembly CFRP sleeve specimen

### III. RESULTS AND DISCUSSIONS

Leak tests were conducted to explore how effective the joints were against the leakage of a high pressure lubricating oil (SAE 40). The specimens of leak test were prepared between aluminum adherends only, but with two kinds of sleeves, GFRP and CFRP. The specimens are addressed as Al-GFRP-Al and Al-CFRP-Al. The glass fiber roving used was 1200 Tex while carbon fiber roving used was of 210 Tex. The thickness of the sleeve was varied depending on the number of passes and the testing was conducted on the dead weight pressure gauge tester using a specially designed attachment as discussed earlier.

#### A. Leak Pressure Test: Al-GFRP-AL

Table 3 shows the experimental results on GFRP specimens (Al-GFRP-Al) with the various numbers of passes, n. Three sets of experiments were conducted for each passes of GFRP specimens.

Table 3: Leak test results for Al-GFRP-Al specimens

Sr. No.	No. of passes	Stiffness Ratio $S_a$	Leakage pressure (bar)			
			Set 1	Set 2	Set 3	Average
1	35	0.239	125	140	150	138.3 ± 12.6
2	45	0.309	140	150	135	141.7 ± 7.6
3	55	0.378	170	190	160	173.3 ± 15.3
4	65	0.445	185	190	190	188.3 ± 2.9
5	75	0.514	195	215	240	216.7 ± 22.5
6	85	0.583	250*	250*	250*	250

\* No leakage

Figure 11 show the relation between the leakage pressure and the number of passes of GFRP specimen (n). The pressure was not allowed to exceed beyond 250 bar to avoid the bursting of aluminum adherend.

It was observed that the specimen of lesser number of passes of glass fiber roving leaked radially out through the GFRP joint near the joint plane while the specimens of higher number of passes leaked through the one of the ends of GFRP sleeve. Figure 12 and Figure 13 illustrates the mode of failure during leakage testing. No leakage of fluid was observed for  $n \geq 85$  (Stiffness ratio,  $S_a \geq 0.583$ ) of Al-GFRP-Al specimen at the fluid pressure of 250 bar.

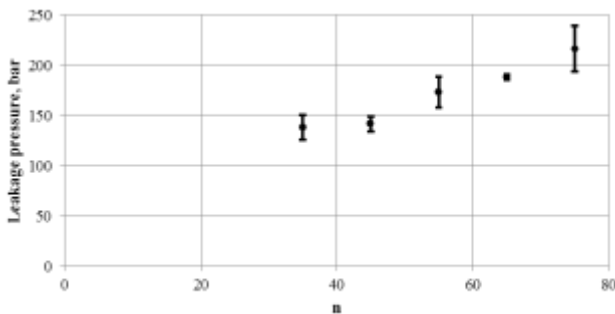


Fig. 11: Leakage pressure vs. number of passes of GFRP specimen (n)

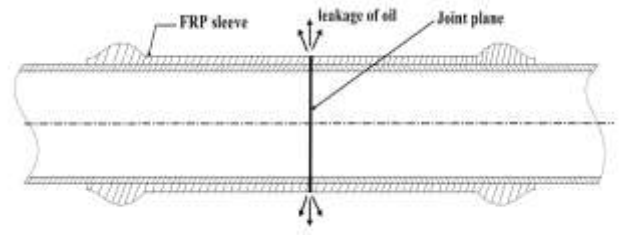


Fig. 12: The oil leakage through the sleeve at the joint plane when the sleeve was thin.

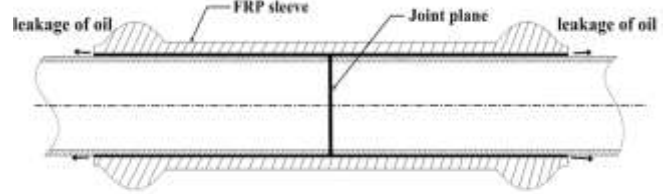


Fig. 13: The oil leakage through the ends (at the leading edge) when the sleeve was thick.

#### B. Leak Pressure Test: Al-CFRP-AL

Similar to experimentation of Al-GFRP-AL specimen, leak tests were conducted for the Al-Al-CFRP-Al specimens for various numbers of passes of carbon fiber roving. Table 4 shows the experimental results on CFRP specimens (Al-CFRP-Al) with the various numbers of passes, n.

Sr. No.	No. of passes	Stiffness Ratio $S_a$	Leakage pressure (bar)			
			Set 1	Set 2	Set 3	Average
1	75	0.251	120	130	130	126.7 ± 4.1
2	100	0.333	175	160	190	175.0 ± 15.0
3	125	0.412	230	200	205	211.7 ± 16.1
4	150	0.502	250*	250*	250*	250

Table 4: Leak test results for Al-CFRP-Al specimens

\* No leakage

Figure 14 show the relation between Leakage pressure and the number of passes of CFRP specimen (n).

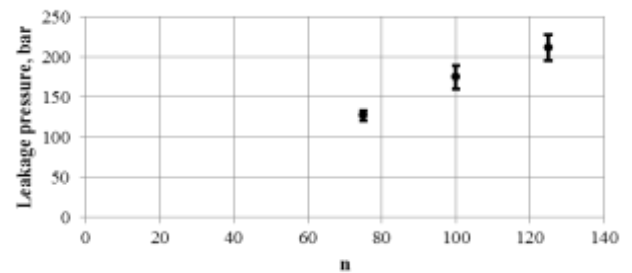


Fig. 14: Leakage pressure vs. number of passes of CFRP specimen (n)

Similar to GFRP specimen test, the pressure was not allowed to exceed beyond 250 bar to avoid the bursting of aluminum adherend as same aluminum material was used. No leakage of fluid was observed for  $n \geq 150$  (Stiffness ratio,  $S_a \geq 0.502$ ) for Al-CFRP-Al specimen at the fluid pressure of 250 bar.

#### IV. CONCLUSION

Leak tests were conducted for the specimens with various numbers of passes to explore how effective the joints were against the leakage of a high pressure lubricating oil (SAE 40). Leak tests were conducted for the two types of specimens Al-GFRP-Al and Al-CFRP-Al with various numbers of passes,  $n$ . The tests were conducted on a dead weight pressure gauge tester using an appropriately designed attachment. The GFRP specimens were found to be leak proof at 250 bar for  $n \geq 85$  (Stiffness ratio,  $S_a \geq 0.583$ ) while the CFRP specimens did not show any leakage of the oil at 250 bar for  $n \geq 150$  (Stiffness ratio,  $S_a \geq 0.502$ ). Thus strength of the CFRP sleeve specimen was found to be more as compare to GFRP sleeve specimen against the leakage. When the FRP sleeve was thin, the fluid leaked radially out at the joint plane. However, when the sleeve was made thick, no leakage was found near the joint plane. The liquid was observed to leak through the one of the ends of the FRP sleeve.

During Leak test, when the pressure inside the aluminium pipe increases hoop stress also increase leading to expansion of aluminium pipe thereby forming the strong matrix of FRP. This formation of strong matrix increases the pressure at which leak occurs i.e. it enhances the results. Results are subjected to room temperature but specimen may fail at low pressure when working temperature is high.

#### REFERENCES

- [1] Kumar P, Singh R K, Kumar R, Joining similar and dissimilar materials with GFRP. *Int J Adhesion & Adhesives*. 27 (2007) 68–76.
- [2] Kumar P and Kumar R, Joining of pipes using FRP - an experimental study, *J Institute of Engineers (India)*. 89 (2008) 16-19.
- [3] Ramkumar J, Singhal A K, Singh R K, Kumar P, Butt joining of similar & dissimilar pipe material by cold joining process. *Ad composite letters*. 16 (2007) 173-79.
- [4] Imanaka M, Nakayama H, Nakamura M, Evaluations of fatigue life of adhesively bonded CFRP pipe/steel rod joints, *Composite SWUZMS*. 31 (1995) 235-41.
- [5] Jiao H, Zhao XL, CFRP strengthened butt-welded very high strength (VHS) circular steel tubes, *Thin-Walled Structures*. 42 (2004) 963–78.
- [6] Fawzia S, Al-Mahaidi R, Zhao X L, Rizkalla S, Strengthening of circular hollow steel tubular sections using high modulus CFRP sheets, *Construction and Building Materials*. 21 (2007) 839–45.
- [7] Zhao X L, Zhang L, State-of-the-art review on FRP strengthened steel structures, *Engineering Structures*. 29 (2007) 1808–23.
- [8] Raykhere S L, Kumar P, Singh R K, Parameswaran V, Dynamic shear strength of adhesive joints made of metallic and composite adherends, *Materials and Design*. 31 (2010) 2102–09. 15
- [9] Ladhwe, R.N., Kumar, P., Singh, K.K. and Sarkar, P.K. ‘Characterization of GFRP butt-joint under tensile and flexural loading.’ *Journal of Composite Material* September 4, 2014. doi: 10.1177/0021998314550220.
- [10] Ladhwe, R.N., Kumar, P., Singh, K.K., Sarkar, P.K. and Ugale, V. ‘Experimental study and numerical analysis of a CFRP butt-joint between the pipes of dissimilar materials.’ *The Journal of Adhesion* November 21, 2014. doi: 10.1080/00218464.2014.972502
- [11] W. Hunfenbach, R.Bohm, “Damage monitoring in pressure vessels and pipelines” 10, 2011
- [12] Agarwal BD and Broutman LJ. *Analysis and Performance of Fiber Composites*. John Wiley & Sons, Inc., New York, 1990.
- [13] Danial Issac M and Ishai Ori. *Engineering Mechanics of Composite Materials*. Oxford University Press, 1994.
- [14] Berhelot Jean-Marie. *Composite Materials-Mechanical Behavior and Structural Analysis*. Springer publication, New York, 1999.